Probability of Missile Generation from Low Pressure Turbines

Non-Proprietary Version

December 2007

Revision History

Revision	Page	Description
0	All	Original Issue

Mitsubishi Heavy Industries, Ltd.
16-5, Konan 2-chome, Minato-ku
Tokyo 108-8215 Japan

Abstract

The purpose of this document and analyses is to show the probability of missile generation from integral low pressure rotors.

Four failure mechanisms are evaluated; destructive overspeed bursting, fracture due to high cycle fatigue, low cycle fatigue and stress corrosion. Stress corrosion cracking was identified to be the dominant mechanism to determine the probability of missile generation.

The probability of missile generation by this mechanism does not exceed 10^{-5} per year even after [ ] of running time. It is concluded that the NRC safety guidelines can be satisfied through the periodic inspection in a proper interval within [ ].

Table of Contents

List of Tables

List of Figures

List of Acronyms

The following list defines the acronyms used in this document.

a	Crack Size in Depth
a_i	Initial Critical Crack Size in Depth
a_{cr}	Critical Crack Size in Depth
F	Flaw Shape Parameter = SQRT (Q/1.21)
FATT	Fracture Appearance Transition Temperature
HCF	High Cycle Fatigue
K_{IC}	Fracture Toughness (of the rotor)
LCF	Low Cycle Fatigue
LP rotor	Low Pressure Turbine Rotor
N	Number of Cycles (ex. Number of Start & Shut-down)
N_f	Number of Cycles of Failure
OS	Over Speed
P_{SCC}	Probability of Missile Generation due to SCC
q_i	Probability of Crack Initiation
q_{cr}	Probability of Flaw Propagation up to Critical Crack Size
q_{OS}	Probability of Reaching Design Overspeed
Q	Flaw Shape Parameter
SCC	Stress Corrosion Cracking
SF	Safety Factor (ex. $\Delta\sigma_{fail}/\Delta\sigma_{peak}$)
T	Temperature
TS	Tensile Strength
YS	Yield Strength
γ	Crack Depth Growth Rate
e	Uncertainty Term
σ	Stress
σ_{fail}	Failure Stress
σ_{ys}	Yield Strength
$\Delta\sigma$	Stress Range
$\Delta\sigma_{al}$	Allowable Stress Range
$\Delta\sigma_{fail}$	Failure Stress Range
$\Delta\sigma_{peak}$	Peak (Maximum) Stress Range
ΔK	Stress Intensity Range
ΔK_{th}	Threshold Stress Intensity Range

1.0 INTRODUCTION

A typical steam turbine for modern nuclear power stations consists of a double flow high pressure element and two or three double flow low pressure elements in tandem. The rotor of the high pressure element generally consists of a single forging with blades being attached in a fashion dependent upon the specific manufacturer's preferences. On the other hand, recently, a larger size of nuclear low pressure rotors has been used to structure together the individual shaft and discs. Each disc is usually shrunk on and keyed to the shaft.

Advancement in steel making technologies and facilities mitigated the restriction for the size of high quality ingot and the size of forging in the manufacturing process of low pressure rotors. This advancement made possible the application of the high quality integral low pressure rotor to the nuclear turbine. The advantage of applying integral low pressure rotors, which are to be applied to US-APWR, is discussed in the following sections.

The purpose of this document is to assess the integrity and safety of US-APWR integral LP rotor designs in order to establish requirements on the nature and frequency of in-service rotor inspections. This assessment is accomplished by evaluating the possibility of a rotor fracture which could lead to bursting and missile generation from the low pressure turbine.

2.0 DESIGN FEATURES

A typical integral rotor is shown in Figure 2-1. A major advantage of this design is the elimination of the disc bores and keyways. Rotors with shrunk-on discs have peak stresses around the locations where the discs are shrunk-on and keyed to the shaft. The elimination of these structures has shifted the location of peak stress from the keyways to blade fastening regions at the rim of the rotor, whose local stress is much lower than that of the shrunk-on discs. Since cracks are likely to occur in high stressed regions, reduction of the peak stress throughout the rotor significantly contributes to the reduction of the rotor burst probability.

In addition to lower local stress throughout the rotor, the integral structure also has the benefit of reduced average tangential stress of the discs and this fact allows us to apply lower yield strength material with traditional safety margins remaining as they are. The integral rotor forgings are heat-treated to obtain minimum yield strengths of [ ] depending upon the requirements of the particular application. Many years of experience and testing of the 3.5% Ni-Cr-Mo-V alloy steel rotor material have demonstrated better ductility, toughness and resistance to stress corrosion cracking at a lower yield strength. These benefits can be important factors to reduce the possibility of turbine missile generation.

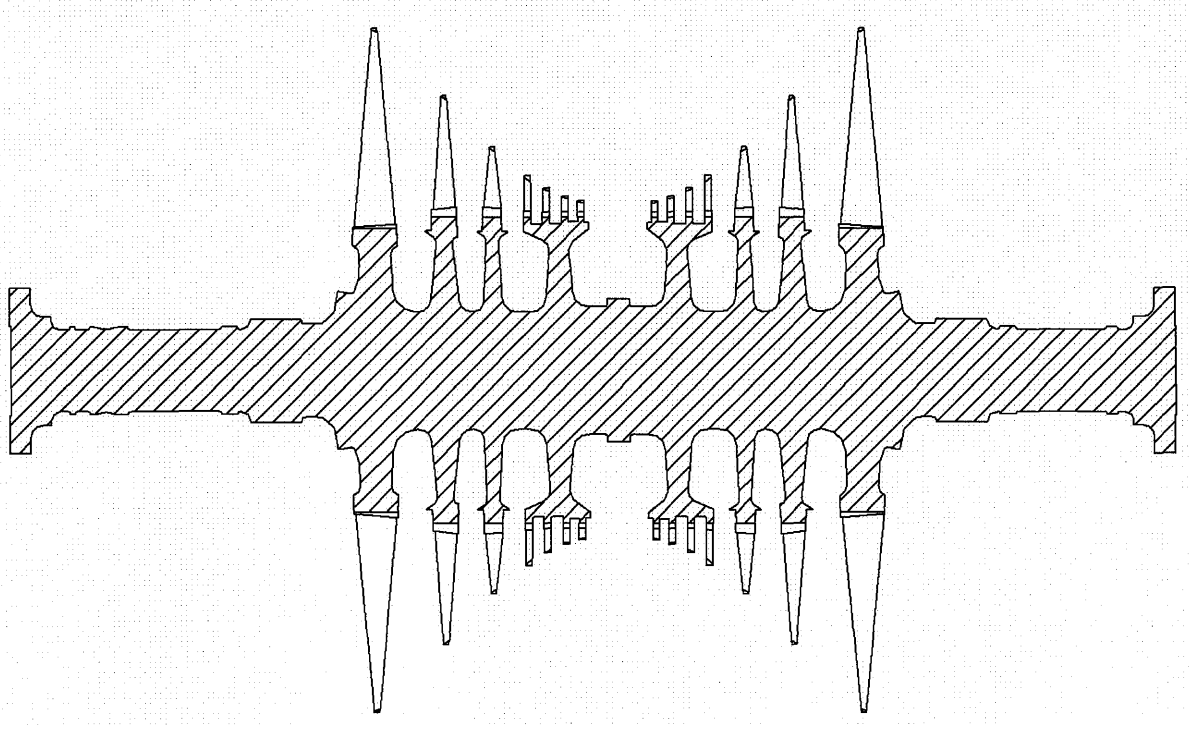

Figure 2-1 Typical Integral Rotor Structure

2.1 Material Feature

In addition to increased capability of manufacturing large size of rotor forgings, improvements in the steelmaking process has resulted in improved toughness, uniformity of properties and reductions in undesirable embrittling elements than were previously achieved.

The specification for integral rotors requires testing at the locations shown in Figure 2.1-1 to confirm uniformity of the rotor. Using these specimens, the tensile test (tensile strength, yield strength, elongation and area reduction) and impact test (absorbed energy, 50% FATT and upper shelf energy) shall be performed and confirm if the required specifications are satisfied.

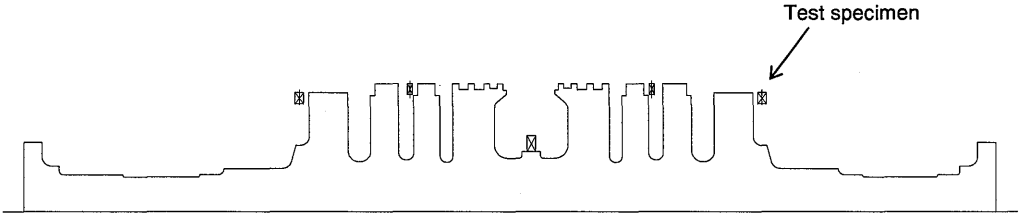

Figure 2.1-1 Typical Integral Rotor Material Test Locations

3.0 PROBABILITY OF MISSILE GENERATION

Four potential failure mechanisms are considered for the assessment of the missile generation probability of an integral low pressure rotor;

1. Ductile burst,

2. Fracture due to high cycle fatigue(HCF),

3. Fracture due to low cycle fatigue(LCF),

4. Fracture due to stress corrosion cracking(SCC).

For the purposes of conservative analyses, a rotor burst is considered sufficient to create a missile although it is recognized that the turbine casing could provide resistance against missiles breaking out to the external. The methodology and results for each of the failure mechanisms are analyzed and discussed in the following sections.

3.1 Ductile Burst

Tests have been performed by a number of investigators in which model turbine discs have been spun to the point of failure. The results demonstrate that ductile failure can be predicted by assuming the average tangential stress equal to the tensile strength of the disc at burst. It becomes possible to calculate the speed at which failure would occur by knowing the stress required for failure. The integral rotor body is divided into individual discs as shown in Table 3.1-1 for this analysis. To be more conservative, it is assumed that failure occurs when the average tangential stress in any individual disc is equal to the [ ] of the disc rather than the tensile strength.

The results of this analysis are summarized in Table 3.1-1. We can conclude from this analysis that ductile bursting of the rotor will not occur until the speed of the rotor is increased to equal or be greater than [ ], although this analysis is conservatively evaluated by using [ ]. Since this is well beyond the design overspeed, the rotor cannot fail by this mechanism unless the [ ]. The probability of this event is therefore determined by the [ ], and periodic rotor inspections have no effect on the probability of failure by this mechanism.

Table 3.1-1 Safety Factors for Ductile Bursting

[redacted]

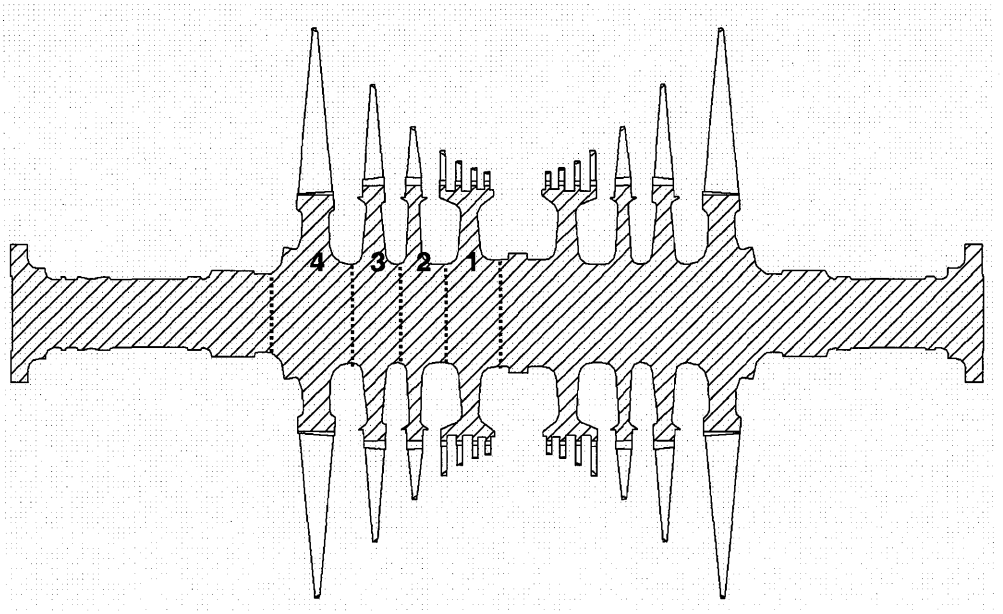

3.2 Fracture Due To High Cycle Fatigue (HCF)

In this scenario it is postulated that a failure can occur from a fatigue crack which propagates in a plane transverse to the rotor axis as a result of cyclic bending loads on the rotor. These loads are developed by gravity forces and by possible misalignment of the bearings. Missile generation by this mechanism is highly unlikely since:

1. Large safety factors used in the design minimize the initiation and propagation of a fatigue crack.

2. A large transverse crack will create eccentricity and the resulting high vibrations will cause the unit to be removed from service before fracture occurs.

In order to assure that the rotor burst by this scenario will not occur during service operation, the following analyses are to be done;

1. Initiation of HCF cracks,

2. Propagation of cracks by HCF.

Initiating a HCF cracks are evaluated by comparing the magnitude of the bending stress with the failure stress σ_{fail}, obtained from a Goodman Diagram and reduced to account for size effects. Table 3.2-1 shows the calculated safety factor against HCF at each surface position of each low pressure rotor. It is seen that [ ] is the location where the minimum safety factor of [ ] is observed, while the safety factor on the same position is big enough to prevent the initiation of cracks due to HCF. These rotors therefore have sufficient strength against the HCF fracture from the viewpoint of crack initiation.

The propagation of a postulated pre-existing crack is evaluated as follows:

The rotors have the threshold stress intensity range ΔK_{th}, for fatigue crack propagation and that is obtained from this relation:

$$(3.1) \quad \Delta K_{th} = F \cdot \Delta\sigma \sqrt{\pi \cdot a}$$

where $\Delta\sigma$ is the alternating bending stress and a is the existing crack size in depth. And the flaw shape parameter F is obtained as below:

$$(3.2) \quad F = \sqrt{Q/1.21},$$

where Q, the flaw shape parameter is also determined by assuming a semi-elliptical crack at the material surface. The number of Q is [ ] when assuming the depth to length ratio of [ ].

For the purpose of conservative analysis and obtaining allowable vibration stress $\Delta\sigma_{al}$, the threshold stress intensity range ΔK_{th} is assumed to be [ ]. Initial crack size, a_i is assumed to be [ ].

(3.3) $$\Delta\sigma_{al} = \Delta K_{th} \cdot \sqrt{\frac{1.21}{Q \cdot \pi \cdot a_i}} = [\quad\quad\quad]$$

By comparing the peak stress with the allowable vibratory stress, in Table 3.2-1, all of the peak stresses $\Delta\sigma_{peak}$ are well below the minimum allowable vibratory stress $\Delta\sigma_{al}$. It is therefore obvious that the rotors have a sufficient safety margin in regard to the propagation of a postulated pre-existing crack.

It is concluded that low pressure rotors have sufficient safety factors against HCF. And periodic in-service inspections for transverse fatigue fractures are not required.

Table 3.2-1 HCF Peak alternating Stresses and Safety Factors due to Gravity Bending and Possible Misalignment of the Bearings

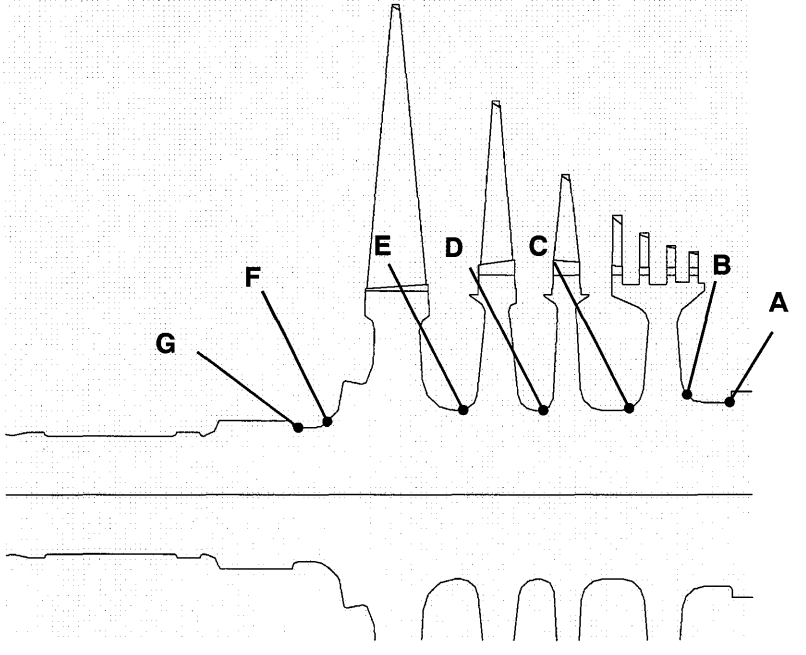

3.3 Fracture Due To Low Cycle Fatigue (LCF)- Startup/Shutdown Cycles

An analysis was carried out to determine the probability of turbine missile generation due to startup-shutdown cycle fatigue crack growth. In this postulated scenario, the failure mechanism is a brittle fracture, where a crack initiates at the center of the rotor and grows to a critical size as a result of speed cycling during the operating life of the turbine.

Such probability of failure depends on the magnitudes and interrelationships of the following six factors:

1. The size of cracks in the bore at the beginning of turbine operation
2. The shape of these cracks
3. The size of the critical crack (dependent on the exposed stresses at running speed or design overspeed and toughness of the rotor)
4. The magnitude of the stress range cycles experienced during the operation of machines

5&6. The two parameters, C_0 and n, in the Paris fatigue crack growth rate equation:

$$\frac{da}{dN} = C_0(\Delta K)^n \tag{3.4}$$

where da/dN is the crack growth rate per cycle, ΔK is the stress intensity range, and n and C_0 are parameters to determine the fatigue crack growth rate which are determined experimentally.

These factors are related to the number of cycles of failure N_f by the equation:

$$N_f = \frac{2}{(n-2)\cdot C_0 \cdot M^{n/2} \cdot \Delta\sigma^n}\left(a_i^{-(n-2)/2} - a_{cr}^{-(n-2)/2}\right) \tag{3.5}$$

where

N_f = The number of cycles to reach critical crack size

M = π/Q

Q = Flaw shape parameter

a_i = Initial largest crack depth

a_{cr} = Critical crack depth

$\Delta\sigma$ = Range of stress cycles in operation.

In the estimation of the probability of rupture by this scenario, both C_0 and n factors

described above are considered to be random variables, and other parameters are conservatively determined. The number of cycles to failure N_f is then dependent on the profile of the above variables. The profiles of the random variables and other parameters are taken as follows:

The flaw shape parameter Q is determined by assuming that a semi elliptical crack with a depth to length ratio of [ ] is formed at the center of the rotor. Such a flaw crack shape parameter would be [ ], which is independent on the stress. Q can be set to be [ ] as a conservative number.

The critical crack size a_{cr} is obtained from the relation:

$$(3.6) \quad a_{cr} = \frac{Q}{\pi}\left(\frac{K_{IC}}{\sigma}\right)^2$$

where K_{IC} is the fracture toughness of the rotor and σ is the stress at rated speed or design overspeed [ ]. The stress σ is [ ] to be [ ], respectively at rated speed and design overspeed. These values are the sum of centrifugal stress and the maximum anticipated thermal stress during start-up cycle. The rotor metal temperature distribution at the rated condition is shown in Figure 3.3-1 for reference.

The fracture toughness K_{IC} of [ ] is applied on this analysis.

The size of the initial crack depth a_i is set to be [ ] under the assumption of [ ] flaw shape, since the inspection procedures used for integral rotor forgings can reliably detect flaws [ ].

The stress range of $\Delta\sigma$ is taken to be a combined stress range occurring during a start-up and shut-down considering centrifugal and thermal stresses as previously discussed.

Profiles of random variables are obtained as follows:

The distribution of C_0 and n were obtained from fatigue crack growth rate data for 3.5% Ni-Cr-Mo-V rotor steel presented in Table 3.3-1.

The values of n and C_0 are assumed to have a normally distributed profile with a mean value of [ ] and standard deviation of [ ] and with a mean value of [ ] and standard deviation of [ ] respectively.

The calculated results in regard to the probability of a LP rotor rupture due to LCF are summarized in Table 3.3-2. The number of start and stops, at which the crack size is increased up to a critical one, is very large.

It takes [ ] of start and stops for the initial cracks to grow up to the critical size with their maximum potential, which corresponds even under the assumption of weekly start and stops for [ ] with [ ] overspeed condition. It is concluded that a low pressure rotor rupture can not actually happen under the actual plant operation.

Table 3.3-1 3.5% Ni-Cr-Mo-V Rotor Steel, n and C_0 Parameters in the Paris Equation:

$$\frac{da}{dN} = C_0(\Delta K)^n$$

[ ]

Table 3.3-2 Probability of Low Pressure Rotor Brittle Rupture due to Low Cycle Fatigue (start-up/shut-down cycle)

[ ]

Figure 3.3-1 Temperature Distributions in the LP Rotor (At Rated Condition)

3.4 Failure Due To Stress Corrosion Cracking (SCC)

An analysis was performed to determine the probability of integral rotor bursting due to SCC. A crack is assumed to initiate at the rim where the stresses are the highest, and propagate inward in radial direction until it reaches the critical crack size before bursting. The probability of rotor fracture due to this failure mechanism is a function of the probability of crack initiation, the rate at which a crack could grow due to stress corrosion, and the critical crack depth that will lead to a burst at either the running speed or the design overspeed. Each of these factors is discussed below.

For this analysis, it is only necessary to consider [ ] on the rotor. [ ] of the LP rotor is exposed to superheated steam and experience has demonstrated that SCC does not occur in dry superheated steam. Experience with built-up rotors has also shown that the probability of cracking and the crack growth rates of the discs beyond the [ ] is so low that it is not necessary to consider them in determining the probability of rotor bursting.

The probability of missile generation due to SCC is expressed as follows:

(3.7) $P_{SCC} = q_i \cdot q_{cr} \cdot q_{OS}$

where, q_i is the probability of crack initiation, q_{cr} is the probability of flaw propagation up to the critical size by SCC, and q_{os} is the probability that the unit will reach design overspeed. For the purpose of conservative evaluation, it is assumed that q_i is regarded as 100%, although we have no experience of finding cracks on integral low pressure rotors in inspections until 2007. q_{os} is also assumed to be 100%, nevertheless it is presumed to be in the order of 10^{-5} under proper inspection and maintenance for turbine valves and the control system.

Thanks to the full integral rotor design without shrunk-on and keyways and to a relatively low yield strength of about [ ], we have no experience of emanating SCC on full integral low pressure rotors. However, probability analysis for rotor failure due to SCC is carried out based on experimental and field data of high yield stress materials for conservative purposes.

3.4.1 Crack Growth Rates

The crack growth rate model used in this analysis is expressed as follows:

(3.8) [ ]

where [

]

The actual numbers used for this analysis are the same as those obtained in the experience for keyway stress corrosion crack growth rate in built-up rotors:

[ ]

[ ]

[ ]

Normal distribution of ε with a mean value of [ ] was used. The distribution of ε was obtained from crack growth rate data for the 3.5% Ni-Cr-Mo-V rotor steel presented in Table 3.4-1. Although these rotors have different mechanical properties from that of the integral rotor, the crack growth rate uncertainty ε can be regarded to be the same because of the same chemical compositions.

The calculations were carried out for [
].

Table 3.4-1 3.5% Ni-Cr-Mo-V Rotor Steel Crack Growth Rate Deviation from Calculation

[ ]

3.4.2 Critical Crack Size

The critical crack depths were obtained for [ ] of integral rotors by using the relationship between fracture toughness and stress intensity, as is done in LCF evaluation in Section 3.3. Critical crack depths were determined at running speed and design overspeed considering stress distribution change along with the crack propagation inward.

3.4.3 Numerical Results

Based on the distribution and variance of crack growth rates and critical crack sizes described in the previous sections, analyses were made to determine the probability in a manner that a crack would grow to the critical size within any time interval, t. This probability of rotor bursting is modified by the number of discs being considered.

The final probability profiles are given in terms of discrete inspection intervals in Table 3.4-2 and are shown in Figure 3.4-1. The results show that the necessary inspection interval to satisfy the requirement of missile generation probability less than 10^{-5} per year is [ ] even under the conservative assumptions incorporated into this analysis.

Table 3.4-2 Probability of Missile Generation (per year) due to Stress Corrosion Cracking

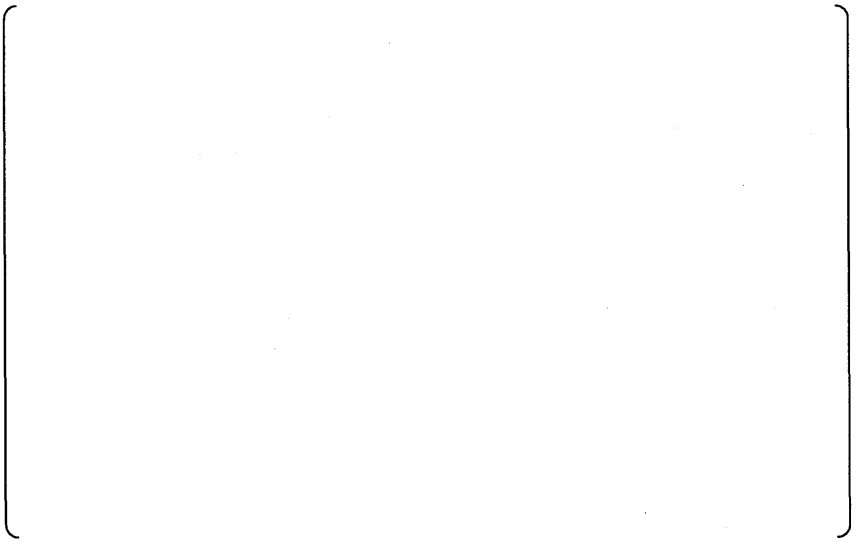

Figure 3.4-1 Probability of Missile Generation (per year) due to Stress Corrosion Cracking

4.0 DISCUSSION AND CONCLUSIONS

Except for the destructive overspeed mechanism, previous discussions demonstrate that the integral low pressure rotor design is unlikely to generate a turbine missile by any of the mechanisms considered in this document and satisfy the requirement in regard to missile generation. The probability of reaching destructive overspeed is primarily dependent upon the [ ]. Detailed discussion on this matter is addressed in Reference 11.

The low pressure rotors are unlikely to burst as a result of HCF since the maximum alternating stress on the rotor is less than its endurance, and the safety factors are more than 3.0. Additional assurances against bursting by this mechanism are derived from;

1. The locations of maximum stress in integral rotors are readily accessible for inspection during normal maintenance,

2. The existence of a large transverse crack is detectable by high vibrations due to rotor unbalance.

It is reasonable to exclude HCF as a controlling mechanism to determine in-service inspection intervals.

Analysis of the LCF mechanism demonstrates that the probability of failure by this scenario is extremely low even under conservative assumptions. Therefore, LCF can be also excluded out of the controlling mechanism for determining inspection intervals.

The SCC has the greatest influence on rotor integrity. The probability of failure by this mechanism is however significantly reduced by the application of integral rotor design. The analysis shows that a running time [ ] may elapse before the first inspection without exceeding the NRC safety guidelines even under highly conservative assumptions. Considering the fact that crack locations are readily accessible during normal turbine inspections and maintenance, it is concluded from the design view point that the NRC safety guidelines can be satisfied by the periodic inspection in a proper interval within [ ].

5.0 REFERENCES

1. S. Kawaguchi, R. Yanagimoto, S. Sawada, and T. Ohhashi, "Historical View of Manufacturing Large Mono-Block Rotor Forgings and Future Outlook", International Forging Conference 1981, Volume 1, May 4-9, 1981.

2. J. M. Barson and S. T. Rolfe, "Correlations Between KIC and Charpy V-Notch Test Results in the Transition Temperature Range", Impact Testing of Metals, ASTM STP 466, 1970, pp. 281-302.

3. Walden, N.E.; Percy, M.J.; and Mellor, P.B., "Burst Strength of Rotating Discs", Proceedings of the Institute of Mechanical Engineers, 1965-66.

4. Peterson, Mochel, Conrad and Gunther, "Large Rotor Forgings for Turbines and Generators", ASME Annual Meeting, November 1955.

5. Robinson, E.L., "Bursting Tests of Steam Turbine Disc Wheels", ASME Annual Meeting, 1943.

6. P. C. Paris, "The Fracture Mechanism Approach to Fatigue", Fatigue – An Interdisciplinary Approach, Proc. 10th Sagamore Army Materials Research Conference, Syracuse University Press, 1964.

7. H. Itoh, T. Momoo, S. Tsukamoto," SCC Suceptibilly of 3.5NiCrMoV Steel in An Actual Low-Pressure Turbine Environment", ICONE-8113, 2000.

8. F. F. Lyle Jr., H. C. Burghard Jr., "Steam Turbine Disc Cracking Experience", EPRI NP-2429-LD RP 1389-5, Vol.1~7, 1982.

9. B. W. Roberts, P. Greenfield, "Stress Corrosion of Steam Turbine Disc and Rotor Steels", CORROSION-NACE Vol. 35, No.9, p.402, 1979.

10. T. Endo, H. Itoh, Y. Kondo, H. Karato, "Material Aspect for the Prevention of Environmentally Assisted Cracking in Low Pressure Turbine", PWR-Vol.21, The Steam Turbine Generator Today: Materials, Flow Path Design, Repair and Refurbishment, 1993.

11. MUAP-07029(R0)-P, Proprietary and MUAP-07029(R0)-NP, Nonproprietary, "Probabilistic Evaluation of Turbine Valve Test Frequency," Revision 0, December 2007.